A New Metastable Three-Dimensional Bismuth Sulfide with Large Tunnels: Synthesis, Structural Characterization, Ion-Exchange Properties, and Reactivity of KBi_3S_5

Timothy J. McCarthy, Troy A. Tanzer,† and Mercouri G. Kanatzidis*,‡

Contribution from the Department of Chemistry and the Center for Fundamental Materials Research, Michigan State University, East Lansing, Michigan 48824

Received April 28, 1994[⊗]

Abstract: The new ternary bismuth sulfide KBi_3S_5 forms from the reaction of Bi in a K_2S_x flux at 300 °C (94% yield). The compound crystallizes in the orthorhombic space group *Pnma* (no. 62) with a = 17.013(5) Å, b = 4.076(2) Å, c = 17.365(4) Å, V = 1204(2) Å^3, and Z = 4 (final R/R_w = 5.1/6.7%), data with $F_o^2 > 3\sigma(F_o^2)$ 782, no. of variables 59, $2\theta_{max} = 50°$. The compound contains an open framework composed of edge-sharing BiS_6 octahedra to form large tunnels which are occupied by K^+ ions fractionally distributed over two sites. The S⋯S distances across the channel range from 9.45−14.02 Å. KBi_3S_5 is a semiconductor with a band-gap of 1.21 eV. It undergoes a structural change upon heating at 520 °C. KBi_3S_5 exhibits topotactic ion-exchange with RbCl to give β-$RbBi_3S_5$ at 350−380 °C. Ion-exchange with aqueous HCl in air forms an oxidized, metastable bismuth sulfide which undergoes endothermic decomposition to Bi_2S_3 at ~140 °C.

Introduction

Although binary bismuth chalcogenide phases have received considerable attention for their excellent thermoelectric properties near room temperature,[1] there has been very little exploratory synthesis of new ternary bismuth chalcogenide phases. Outside of the well-known NaCl-type $ABiQ_2$ (A = Li, Na, K; Q = S, Se)[2] compounds, the only other phases that have been fully characterized structurally are $CsBi_3S_5$,[3] $RbBi_3S_5$,[4] $Tl_4Bi_2S_5$,[5] α-(β-)$BaBi_2S_4$,[6] $Cs_3Bi_7Se_{12}$,[7] $Sr_4Bi_6Se_{13}$,[8] and $BaBiSe_3$.[9] These compounds have been prepared at high temperature by direct combination of the elements or alkali carbonates with Bi and S. In addition, mixed Bi/transition metal/Q (Q = S, Se) solid solution systems have been investigated including $Cu_{1+3x}Bi_{5-x}Q_8$[10] and $Mn_{1-x}Bi_{2+y}Q_4$.[11] Several naturally occurring bismuth sulfosalts, including $PbBi_2S_4$ (galenobismuthite)[12] and $PbCu_4Bi_5S_{11}$,[13] have also been observed. When we consider the structural diversity that can result from the manifestation of the inert lone pair of electrons on Bi^{3+} and from the variable coordination preference of this ion, it becomes apparent that further work in this area is warranted. Recently, we reported on three new ternary bismuth chalcogenides that display a wide range of structural diversity.[14] Thus, while β-$CsBiS_2$ possesses a linear chain structure with corner sharing BiS_3 trigonal pyramids, γ-$CsBiS_2$ forms a layered superstructure of $RbBiS_2$. In $K_2Bi_8Se_{13}$, layers of $BiSe_6$ octahedra are connected by $BiSe^5$ square pyramidal units to form a three-dimensional network with K^+ ions located in channels. Both γ-$CsBiS_2$ and $K_2Bi_8Se_{13}$ exhibit high thermopower and reasonably high n-type electrical conductivity. In an effort to expand this very interesting chemistry, we continued our investigations of the reactivity of Bi in K_2S_x fluxes. The alkali metal polychalogenide flux method has proven to be an extremely useful low temperature route to access novel compounds.[15,16] In this paper, we report on KBi_3S_5, a novel compound with a three-dimensional structure with surprisingly large tunnels for a chalcogenide compound, and with topotactic ion-exchange properties.

The possibility of open metal chalcogenide framework structures that combine the utility of microporous oxides with the useful electronic properties of metal chalcogenides to form a new class of microporous chalcogenides is intriguing. Bedard and co-workers reported the hydrothermal synthesis of several tin sulfides that display microporous activity after partial removal of the occluded template.[17] Other open chalcogenide frameworks were reported in the antimony sulfide system using the hydrothermal method.[18] Recently, a novel molten salt approach using $(Ph_4P)_2Se_x$ fluxes at 200 °C was shown to give

† NSF Summer Research Program in Solid State Chemistry.

‡ Camille and Henry Dreyfus Teacher Scholar 1993−1995.

⊗ Abstract published in *Advance ACS Abstracts,* January 1, 1995.

(1) (a) Rowe, D. M.; Bhandari, C. M. *Modern Thermoelectrics*; Holt, Rinehart and Winston: London, 1983; p 103. (b) Borkowski, K.; Przyluski, J. *J. Mat. Res. Bull.* **1987**, *22*, 381−387.

(2) (a) Boon, J. W. *Recl. Trav. Chim. Pays-Bas* **1944**, *63*, 32. (b) Glemser, O.; Filcek, M. *Z. Anorg. Allg. Chem.* **1955**, *279*, 321−323. (c) Gattow, G.; Zemann, J. *Z. Anorg. Allg. Chem.* **1955**, *279*, 324−327.

(3) Kanishcheva, A. S.; Mikhailov, J. N.; Lazarev, V. B.; Trippel, A. F. *Dokl. Akad. Nauk, SSSR (Kryst.)* **1980**, *252*, 96−99.

(4) Schmitz, D.; Bronger, W. *Z. Naturforsch.* **1974**, *29b*, 438−439.

(5) Julien-Pouzol, M.; Jaulmes, S.; Laruelle, P. *Acta. Crystallogr.* **1979**, *B35*, 1313−1315.

(6) Aurivillius, B. *Acta Chem. Scand.* **1983**, *A37*, 399−407.

(7) Cordier, G.; Schäfer, H.; Schwidetzky, C. *Rev. Chim. Miner.* **1985**, *22*, 676−683.

(8) Cordier, G.; Schäfer, H.; Schwidetzky, C. *Rev. Chim. Miner.* **1985**, *22*, 631−638.

(9) Volk, K.; Cordier, G.; Cook, R.; Schäfer, H. *Z. Naturforsch.* **1990**, *35b*, 136−140.

(10) Liautard, B.; Garcia, J. C.; Brun, G.; Tedenac, J. C.; Maurin, M. Eur. *J. Solid State Inorg. Chem.* **1990**, *27*, 819−830.

(11) Lee, S.; Fischer, E.; Czerniak, J.; Nagasundaram, N. *J. Alloys and Compounds* **1993**, *197*, 1−5.

(12) Iitaka, Y.; Nowacki, W. *Acta Crystallogr.* **1962**, *15*, 691−698.

(13) Kupcik, V.; Makovicky, E. *N. Jb. Miner. Mh.* **1968**, *7*, 236−237.

(14) McCarthy, T. J.; Ngeyi, S.-P.; Liao, J.-H.; DeGroot, D.; Hogan, T.; Kannewurf, C. R.; Kanatzidis, M. G. *Chem. Mater.* **1993**, *5*, 331−340.

(15) (a) Kanatzidis, M. G. *Chem. Mater.* **1990**, *2*, 353−363. (b) Kanatzidis, M. G.; Park, Y. *J. Am. Chem. Soc.* **1990**, *111*, 3767−3769. (c) Kanatzidis, M. G.; Park, Y. *Chem. Mater.* **1990**, *2*, 99−101. (d) Park, Y.; Kanatzidis, M. G. *Angew. Chem., Int. Ed. Engl.* **1990**, *29*, 914−915.

(16) (a) Sunshine, S. A.; Kang, D.; Ibers, J. A. *J. Am. Chem. Soc.* **1987**, *109*, 6202−6204. (b) Kang, D.; Ibers, J. A. *Inorg. Chem.* **1989**, *27*, 549−551.

(17) Bedard R. L.; Wilson, S. T.; Vail, L. D.; Bennett, E. M.; Flanigen, E. M. *Zeolites: Facts, Figures, Future*; Jacobs, P. A., van Sonten, R. A., Eds.; 1989, p 275.

(18) Parise, J. B. *Science* **1991**, *251*, 293−294.

0002-7863/95/1517-1294$09.00/0

Table 1. Solid State Reactions of KBi_3S_5 with Alkali Metal Halides

temp, (°C)	NaCl	RbCl	CsCl
197	no reaction	no reaction	no reaction
297	$NaBiS_2 + Bi_2S_3$	$Rb_xK_{1-x}Bi_3S_5$[a]	γ-$CsBiS_2$
347	$NaBiS_2 + Bi_2S_3$	β-$RbBi_3S_5$[b]	γ-$CsBiS_2$
384		β-$RbBi_3S_5$[b]	γ-$CsBiS_2$ + phase[c]
400		α-$RbBi_3S_5$	γ-$CsBiS_2$ + phase

[a] EDS analysis gave $Rb_{0.54}K_{0.46}Bi_{3.1}S_{5.6}$. [b] Topotactic ion-exchange. [c] EDS analysis gave $Cs_{1.0}Bi_{3.3}S_{5.1}$ (needles) and $Cs_{1.0}Bi_{2.5}S_{3.5}$ (hexagonal plates).

$(Ph_4P)[M(Se_6)_2]$ (M = Ga, In, Tl).[19] The open polymeric framework in these compounds consists of tetrahedral M^{3+} centers and bridging Se_6^{2-} ligands that form an extended structure in two dimensions with Ph_4P^+ cations residing within the layers.

Experimental Section

Reagents. Chemicals in this work were used as obtained from commercial sources. All manipulations were carried out under a dry nitrogen atmosphere in a Vacuum Atmospheres Dri-Lab glovebox. For the preparation of K_2S we used a modified literature procedure.[20]

Potassium Sulfide, K_2S. An amount of 2.460 g (0.077 mol) of sulfur and 6.00 g (0.153 mol) of freshly sliced potassium metal were added to a 250-mL round-bottom flask. A 150 mL volume of liquid ammonia was condensed into the flask at −78 °C (dry ice/acetone) under nitrogen to give a light blue solution. The NH_3 was removed by evaporation under a flow of nitrogen as the bath slowly warmed to room temperature. The pale yellow solid (99% yield) was dried under vacuum overnight, flame-dried, and ground to a fine powder with a mortar and pestle.

Potassium Pentasulfido-tribismuthate(III), KBi_3S_5. The reaction of 0.052 g (0.25 mmol) of Bi, 0.072 g (0.65 mmol) of K_2S and 0.096 g (3.0 mmol) of S in an evacuated Pyrex tube at 300 °C for 5 days, followed by cooling at 4 °C/h to 120 °C and then to room temperature in 1 h, afforded small dark gray needles (94% yield, based on Bi metal). The product, stable with respect to water and air, was isolated by dissolving the excess K_2S_x with methanol under inert atmosphere. Semiquantitative microprobe analysis on single crystals gave $K_{1.4}Bi_{2.8}S_{5.2}$ (average of three data acquisitions). Far-IR (CsI matrix) gave a broad absorbance from 260 to 158 cm^{-1}. Raman spectroscopy gave a strong, broad shift at 267 cm^{-1}.

$(H_2O)Bi_3S_{4.5}(S_8)_{0.06}$. The stirring of 0.200 g (0.242 mmol) of finely ground KBi_3S_5 in a solution of 0.5 M HCl (30 mL), at room temperature in air, afforded a microcrystalline product with the same dark gray color as the starting material. The product was filtered and washed with distilled water, ethanol, and ether. Varying the reaction time (0.5−66 h) and lowering the temperature to 0 °C did not influence the final result. Extensive semiquantitative (EDS) microprobe analyses were performed on the crystallites from several reaction products, giving a K/Bi ratio of 0.01−0.03,[21] suggesting that virtually all K^+ was removed.

β-Rubidium Pentasulfido-tribismuthate(III), β-$RbBi_3S_5$. An amount of 0.042 g (0.051 mmol) of KBi_3S_5 was heated with excess RbCl in a 1:100 ratio in an evacuated Pyrex tube at 350−380 °C for 2 days. After cooling to room temperature over 6 h, the product was washed with distilled water, MeOH, and ether. Semiquantitative (EDS) microprobe analysis on single crystals gave $Rb_{1.0}Bi_{3.5}S_{6.0}$ (average of three data acquisitions) suggesting that virtually all K^+ was removed.

Solid State Reactions with Alkali Metal Chlorides. KBi_3S_5 (0.042 g, 0.051 mmol) was heated with excess ACl (A = Na, Rb, Cs) in a 1:100 ratio in an evacuated Pyrex tube at 200−400 °C for 2 days. After cooling to room temperature over 6 h, the product was washed with distilled water, MeOH, and ether. Details of the reaction conditions are given in Table 1.

The homogeneity of KBi_3S_5 was confirmed by comparing the observed and calculated X-ray powder diffraction patterns. The d_{hkl} spacings observed for the bulk materials were compared and found to be in agreement with the d_{hkl} spacings calculated from the single crystal data using the program POWD10.[22] The results are shown in Table 2.

Table 2. Calculated and Observed X-ray Powder Diffraction Patterns for KBi_3S_5

hkl	$d_{(calc)}$, Å	$d_{(obsd)}$, Å	I/I_{max} (obsd)
101	12.15	12.13	78
002	8.68	8.70	4
200	8.51	8.50	10
202	6.08	6.07	51
103	5.48	5.48	5
301	5.39	5.38	13
303	4.13	4.13	4
303	4.05	4.04	8
402	3.82	3.81	14
112, 211	3.61, 3.60	3.60	11
304	3.45	3.45	42
105	3.40	3.40	37
013	3.33	3.34	14
113	3.27	3.28	6
311	3.25	3.25	12
205	3.22	3.22	25
502	3.17	3.16	11
312	3.09	3.09	5
404	3.04	3.04	6
410	2.94	2.94	13
411, 006	2.90, 2.89	2.90	35
106	2.85	2.85	100
511	2.58	2.58	4
215	2.52	2.52	4
514	2.238	2.238	4
316	2.179	2.179	6
108	2.153	2.153	10
801	2.111	2.106	6
515	2.088	2.087	12
416	2.063	2.063	6
020	2.038	2.039	6
606	2.025	2.023	4
507	2.005	2.005	4
317	1.985	1.986	10
615	1.934	1.933	5
714	1.881	1.881	8
218	1.869	1.869	5
517, 422	1.799, 1.798	1.799	4
423	1.752	1.752	4
119, 904	1.735, 1.733	1.734	9
608	1.724	1.723	8
126	1.658	1.660	8
2011	1.552	1.552	4

Physical Measurements. The FT-IR spectrum of KBi_3S_5 was recorded as a solid in a CsI matrix. The sample was ground with dry CsI into a fine powder, and a pressure of about seven metric tons was applied to the mixture to make a translucent pellet. The spectra were recorded in the far-IR region (600−100 cm^{-1}) with the use of a Nicolet 740 FT-IR spectrometer. The mid-IR spectra (4000−350 cm^{-1}) were recorded as a solid in a KBr matrix. Raman spectra were recorded at room temperature with a Nicolet FT-Raman 950 spectrometer.

Semiquantitative microprobe analysis of the compounds was performed with a JEOL JSM-35C scanning electron microscope (SEM) equipped with a Tracor Northern Energy Dispersive Spectroscopy (EDS) detector. Data were acquired using an accelerating voltage of 20 kV and a 1−2 min accumulation time.

Optical diffuse reflectance measurements were made at room temperature with a Shimadzu UV-3101PC double beam, double-monochromator spectrophotometer. The instrument was equipped with an integrating sphere and controlled by a personal computer. The measurement of diffuse reflectivity can be used to obtain values for the band gap which agree rather well with values obtained by absorption measurements from single crystals of the same material. The digitized spectra were processed using the Kaleidagraph software program. $BaSO_4$ powder was used as reference (100% reflectance). Absorption data were calculated from the reflectance data using the Kubelka−

(19) Dhingra, S.; Kanatzidis, M. G. *Science* **1992**, *258*, 1769−1772.
(20) Feher, F. *Handbuch der Praparativen Anorganischen Chemie*; Brauer, G., Ed.; Ferdinand Enke: Stuttgart, Germany, 1954; pp 280−281.

Munk function[23]

$$\alpha/S = \frac{(1-R)^2}{2R}$$

R is the reflectance at a given wavelength, α is the absorption coefficient, and S is the scattering coefficient. The scattering coefficient has been shown to be practically wavelength independent for particles larger than 5 μm which is smaller than the particle size of the samples used here.[23a,b] The E_g value is extracted from the $(\alpha/s)^2$ vs energy plot. The E_g is taken as the point where the extrapolated linear portion of the plot intersects the energy axis at $(\alpha/s)^2 = 0$.

Thermogravimetric analysis (TGA) was performed with a computer-controlled Shimadzu TGA-50. The samples were heated in a quartz cup from room temperature to 330 °C at a heating rate of 3 °C/min under a nitrogen flow rate of 57 mL/min.

Differential scanning calorimetry (DSC) was performed with a computer-controlled Shimadzu DSC-50 thermal analyzer under a nitrogen atmosphere at a flow rate of 35 mL/min. The samples were crimped in an aluminum pan inside a nitrogen-filled glovebox. The pan was placed on the sample side of the DSC-50 detector, and an empty aluminum pan of equal mass was crimped and placed on the reference side. The samples were heated to the desired temperature at 5 °C/min. The reported DSC temperatures are peak temperatures with a standard deviation of 0.2 deg. The adopted convention in displaying data is exothermic peaks occur at positive heat flow while endothermic peaks occur at negative heat flow.

Differential thermal analysis (DTA) was performed with a computer-controlled Shimadzu DTA-50 thermal analyzer. The ground single crystals (~10.0 mg total mass) were sealed in quartz ampules under vacuum. An empty quartz ampule of equal mass was sealed and placed on the reference side of the detector. The samples were heated to the desired temperature at 20 °C/min and then isothermed for 10 min followed by cooling at 10 °C/min to 200 °C and finally by rapid cooling to room temperature. Indium (reported mp 156.6 °C) and antimony (reported mp 630.9 °C) served as calibration standards. The reported DTA temperatures are peak temperatures. The DTA samples were examined by powder X-ray diffraction after the experiments.

Mass spectrometry was performed with a VG Instruments Trio-1000 mass spectrometer. The solid samples were heated at 5 °C/min. to 300 °C with a solid probe.

X-ray Crystallography. KBi_3S_5 was examined by X-ray powder diffraction for the purpose of phase purity and identification. Accurate d_{hkl} spacings (Å) were obtained from the powder patterns recorded on a Rigaku Rotaflex Powder X-ray diffractometer with Ni filtered Cu Kα radiation operating at 45 kV and 100 mA. The data were collected at a rate of 1.0 deg/min.

The variable temperature powder XRD experiment was performed with the instrument described above. The instrument was equipped with a temperature controller, and the experiment was carried out under nitrogen flow with an enclosed sample compartment. The data were collected at a rate of 2.4 deg/min. The sample was heated to 65 °C and was allowed to equilibrate for 30 min before the XRD was taken. The sample was then heated in 20 °C increments with 30 min equilibration times at each step. The final XRD was taken at 145 °C.

Structure Solution of KBi_3S_5. A crystal with dimensions 0.50 × 0.10 × 0.10 mm was mounted on a tip of a glass capillary. Intensity data were collected using the $\omega-2\theta$ scan mode on a Rigaku AFC6S four-circle automated diffractometer equipped with a graphite-crystal monochromator. The stability of the crystal was monitored by measuring three standard reflections periodically (every 150 reflections) during the course of data collection. No crystal decay was detected. An empirical absorption correction based on ψ scans was applied to the data.

Table 3. Summary of Crystallographic and Structure Analysis Data for KBi_3S_5[a]

formula	KBi_3S_5
fw	826.34
a, Å	17.013(5)
b, Å	4.076(2)
c, Å	17.365(4)
α, deg	90.00
β, deg	90.000
γ, deg	90.000
Z; V, Å^3	4; 1204(2)
λ	0.71073 (Mo Kα)
space group	*Pnma* (no. 62)
D_{calcd}, g/cm^3	4.56
μ, cm^{-1}	447 (Mo Kα)
$2\theta_{max}$, deg	50 (Mo Kα)
temp, °C	23
final R/R_w, %	5.1/6.7
total data measd	1311
total unique data	1311
data with $F_o^2 > 3\sigma(F_o^2)$	782
no. of variables	59

[a] $R = \sum(|F_o| - |F_c|)/\sum|F_o|$; $R_w = \{\sum w(|F_o| - |F_c|)^2/\sum w|F_o|^2\}^{1/2}$.

The space group was determined to be *Pnma* (no. 62), and a solution was found using the automated direct methods function in the SHELXS86 program[24] and refined by full-matrix, least-squares techniques of the TEXSAN package of crystallographic programs.[25] Three bismuth atoms, five sulfur atoms, and a potassium atom were located. Each of the nine atoms resides on a mirror plane. Inspection of the difference Fourier map revealed a significant electron density peak at a distance from S reasonable for K atoms. This peak was assigned to a second K atom which also resided on a mirror plane. Assuming Bi^{3+} and S^{2-}, electroneutrality dictates that only one K^+ atom should be found. After least squares refinement, the isotropic temperature factor for K(2) was rather high at 14.0 Å^2. The occupancy and the temperature factor of this atom were refined to give values of 0.23 and 8.4 Å^2, respectively. At this stage, a disorder model $K(1)_{1-x}K(2)_xBi_3S_5$ seemed to be reasonable. The occupancies of K(1,2) were constrained to 0.5 then refined. Least squares refinement of this model resulted in a occupancy value of 0.39 and a temperature factor of 1.67 for K(1) which decreased from 2.48. K(2) gave a occupancy of 0.11 and a temperature factor of 1.62 which decreased from 8.4. A DIFABS correction was applied to the isotropically refined data.[26] K(2) was refined isotropically because of its small occupancy, while the rest of the atoms were refined anisotropically to give a final $R/R_w = 5.1/6.7$. All calculations were performed on a VAXstation 3100/76 computer. Inspection of rotation photographs of KBi_3S_5 crystals around all the unit cell axes did not reveal the presence of superlattice. The complete data collection parameters and details of the structure solution and refinement for KBi_3S_5 are given in Table 3. The atomic coordinates, average isotropic temperature factors, and their estimated standard deviations for KBi_3S_5 are given in Table 4.

Results and Discussion

Synthesis and Spectroscopy. The synthesis of KBi_3S_5 was accomplished by dissolving Bi in excess $K_2S_{5.6}$ flux at 300 °C followed by isolation in degassed methanol. Dissolving Bi in a slightly more basic flux of $K_2S_{5.3}$ affords KBi_3S_5 and a small amount of impurity phase. Increasing the Lewis basicity further with K_2S_x ($x = 3.7-4.3$) at 300 °C results in the formation of

(21) Also confirmed by atomic absorption analysis performed by Oneida Research Services, Inc. on one of our reaction products as a check for our SEM-EDS elemental analysis results.

(22) Smith, D. K.; Nichols, M. C.; Zolensky, M. J. E. POWD10: A Fortran IV program for calculating X-ray powder diffraction pattern, version 10; Pennsylvania State University: 1983.

(23) (a) Wendlandt, W. W.; Hecht, H. G. *Reflectance Spectroscopy*; Interscience Publishers: 1966. (b) Kotüm, G. *Reflectance Spectroscopy*; Springer Verlag: New York, 1969. (c) Tandon, S. P.; Gupta, J. P. *Phys. Stat. Sol.* **1970**, *38*, 363−367.

(24) Sheldrick, G. M. In *Crystallographic Computing 3*; Sheldrick, G. M.; Kruger, C.; Doddard, R., Eds.; Oxford University Press: Oxford, England, 1985; pp 175−189.

(25) TEXSAN: Single Crystal Structure Analysis Software, Version 5.0, 1989. Molecular Structure Corporation: The Woodlands, TX 77381, 1989.

(26) Walker, N.; Stuart, D. *Acta Crystallogr.* **1983**, *39A*, 158−166.

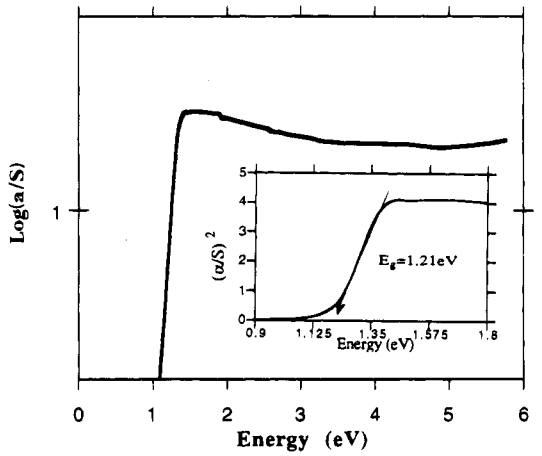

Figure 1. Optical absorption spectrum of KBi_3S_5. Inset shows an expanded $(\alpha/S)^2$ vs energy plot.

β-$KBiS_2$.[27] The synthesis is also complicated by the narrow temperature window (~290−310 °C) in which the compound forms. Below 290 °C, a poorly crystalline KBi_3S_5 phase results. We note that a phase claiming to have the stoichiometry KBi_3S_5 has been reported in high temperature phase diagram studies in the Bi_2S_3−K_2S system, but the powder X-ray diffraction pattern does not resemble that of our compound.[28] Under similar conditions, the attempted synthesis of the Rb^+ analog resulted in the formation of the nonisostructural $RbBi_3S_5$[4] and Bi_2S_3.

A direct combination reaction between Bi_2S_3 and K_2S (3:1) at 325 and 520 °C (for 1 week) was performed to determine if KBi_3S_5 could be isolated in the absence of a flux. However, the product was identified, by powder X-ray diffraction, to be only a mixture of Bi_2S_3 and β-$KBiS_2$. A third, unidentified phase was also detected in the reaction at 520 °C. This experiment confirms the necessity of the molten salt method as a route to KBi_3S_5.

Far-IR spectroscopy of KBi_3S_5 shows a very broad absorption starting at 260 and peaking at 158 cm^{-1}. The Raman spectrum shows a broad shift at 267 cm^{-1}. These peaks are probably due to the Bi−S stretching vibrations. The similarity of the various BiS_6 octahedra in KBi_3S_5 further complicates the assignments due to extensive overlap of Bi−S absorptions.

KBi_3S_5 was found to be a semiconductor with a high resistivity at room temperature of 10^8 Ω·cm. This is consistent with the fact that the material is electron precise.

The optical properties of KBi_3S_5 were assessed by studying the UV−vis-near/IR reflectance spectra. The spectra confirm the semiconducting nature of the material by revealing the presence of a well defined optical gap as shown in Figure 1. The compound exhibits a steep absorption edge from which the band-gap, E_g, can be assessed at 1.21 eV. This transition is determined from a $(\alpha/S)^2$ vs E plot to be direct in character, and it is due to charge transfer from the primarily sulfur-based valence band to the primarily Bi-based conduction band. The E_g of the isomorphous β-$RbBi_3S_5$ (vide infra) was found to be very similar at 1.18 eV. These band-gap values lie in the optimum range for solar energy absorption and point to possible photoconductivity response with visible light irradiation. By comparison, the corresponding band-gap of Bi_2S_3 is 1.3 eV which has been shown to possess photovoltaic properties.[29]

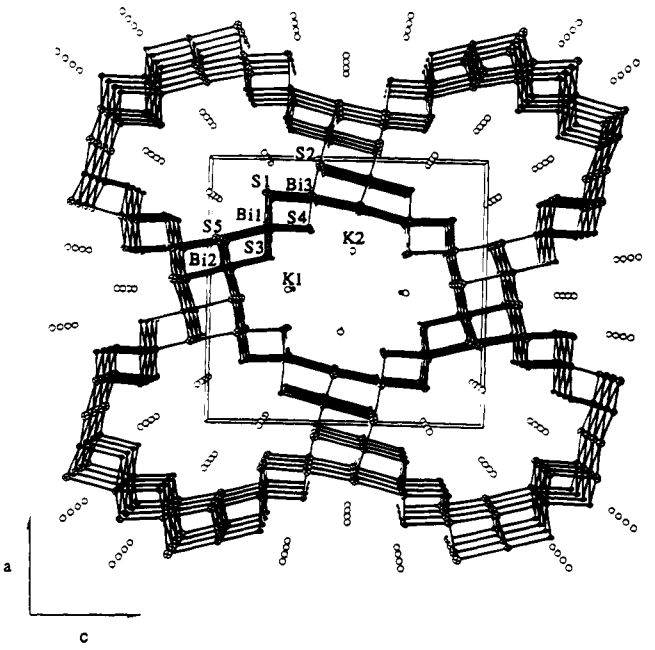

Figure 2. The three-dimensional structure of KBi_3S_5 viewed down the b-axis. The shaded ellipsoids are Bi atoms and the open circles represent K atoms.

Table 4. Fractional Atomic Coordinates and B_{eq} Values[a] for KBi_3S_5 with Estimated Standard Deviations in Parentheses

atom	x	y	z	B_{eq}, Å²
Bi(1)	0.2380(1)	1/4	0.7111(1)	1.40(8)
Bi(2)	0.0831(1)	−1/4	0.5717(1)	1.25(8)
Bi(3)	0.3433(1)	−1/4	0.8743(1)	1.76(9)
K(1)[b]	0.5019(7)	−3/4	0.7041(8)	1.2(5)
K(2)[c]	0.148(3)	1/4	0.018(3)	1.7(9)
S(1)	0.3535(7)	−1/4	0.7162(7)	1.6(6)
S(2)	−0.0363(8)	−3/4	0.6022(7)	1.9(6)
S(3)	0.1235(6)	−1/4	0.7194(6)	1.1(5)
S(4)	0.2325(6)	1/4	−0.1369(9)	1.3(5)
S(5)	0.1894(7)	1/4	0.5393(7)	1.7(5)

[a] B values for anisotropically refined atoms are given in the form of the isotropic equivalent displacement parameters defined as $B_{eq} = (4/3)[a^2B(1,1) + b^2B(2,2) + c^2B(3,3) + ab(\cos\gamma)B(1,2) + ac(\cos\beta)B(1,3) + bc(\cos\alpha)B(2,3)]$. [b] 78% occupied. [c] 22% occupied.

Description of Structure. KBi_3S_5 crystallizes in a different structure type than α-$RbBi_3S_5$[4] or $CsBi_3S_5$.[3] The structure, shown in Figure 2 is built up from edge-sharing BiS_6 octahedra forming a three-dimensional $[Bi_3S_5]^-$ framework. A striking feature of this framework is the presence of large parallel tunnels running along the b-axis. The tunnels are composed of 20-membered rings of alternating Bi and S atoms with S···S distances across the tunnels ranging from 9.45 Å (S(1)−S(1′)) to 14.02 Å (S(2)−S(2′)). The K^+ ions reside in the tunnels and are fractionally distributed over two crystallographic sites with similar coordination environments. The disorder associated with the K^+ ions seems necessary to stabilize the structure. Selected bond distances and bond angles for KBi_3S_5 are given in Table 5. The coordination geometry of the sulfur atoms varies. While S1, S3, and S4 are each bonded to three Bi atoms in a pyramidal geometry, the bonding of S2 and S5 is less common. Atom S2 binds to five Bi atoms in a square planar geometry. If the ionic interaction of K1 with this sulfur atom is taken into account, then the S2 site is described as octahedral.

(27) This phase is isostructural to $RbBiS_2$ as evidenced by powder X-ray diffraction.

(28) Berul, S. I.; Lazarev, V. B.; Trippel, A. F.; Buchikhina, O. P. *Russ. J. Inorg. Chem.* **1977**, *22(9)*, 1390−1393.

(29) Bube, R. H. *Photoconductivity of Solids*; John Wiley and Sons, Inc.: 1960; pp 233−235.

Table 5. Selected Distances (Å) and Angles (deg) in KBi_3S_5 with Standard Deviations in Parentheses[a]

Bi(1)−S(1)	2.833(8) × 2	S(1)−Bi(1)−S(5)	102.5(3)
Bi(1)−S(3)	2.823(7) × 2	S(4′)−Bi(1)−S(5)	162.5(3)
Bi(1)−S(4′)	2.64(1)	Bi(1)−S(1)−Bi(1′)	92.0(3)
Bi(1)−S(5)	3.10(1)	Bi(1)−S(1)−Bi(3)	89.3(3)
Bi(1)−S (mean)	2.8(1)		
Bi(2)−S(2)	2.925(9) × 2	S(2)−Bi(2)−S(3)	179.8(3)
Bi(2)−S(5)	2.782(8) × 2	Bi(2)−S(2)−Bi(2)	88.3(3)
Bi(2)−S(2′)	3.12(1)		
Bi(2)−S(3)	2.66(1)	S(1)−Bi(3)−S(5)	172.6(3)
Bi(2)−S (mean)	2.8(2)	Bi(3)−S(4)−Bi(3′)	94.2(3)
Bi(3)−S(2)	2.919(9) × 2	K(1)−S(1)	3.25(1)
Bi(3)−S(4)	2.783(7) × 2	K(1)−S(1′)	3.25(1)
Bi(3)−S(1)	2.75(1)	K(1)−S(2)	3.43(2)
Bi(3)−S(5)	2.92(1)	K(1)−S(3)	3.19(1)
Bi(3)−S (mean)	2.85(8)	K(1)−S(3′)	3.19(1)
		K(1)−S (av)	3.3(1)
Bi(1)−Bi(1′)	4.076(2)		
Bi(1)−Bi(2)	4.119(2)	K(2)−S(1)	3.44(5)
Bi(1)−Bi(3)	3.923(2)	K(2)−S(4)	3.05(5)
Bi(2)−Bi(3′)	4.186(3)	K(2)−S(5)	3.46(4)
Bi(2)−Bi(3″)	4.180(2)	K(2)−S(5′)	3.46(4)
Bi−Bi (mean)	4.1(1)	K(2)−S (av)	3.3(2)

[a] The estimated standard deviations in the mean bond lengths and the mean bond angles are calculated by the equations $\sigma l = \{\sum n(l_n - l)^2/n(n-1)\}^{1/2}$, where l_n is the length (or angle) of the nth bond, l the mean length (or angle), and n the number of bonds.

Atom S5 is bonded to four Bi atoms in a see-saw geometry with two K2 atoms completing an octahedral geometry. The coordination environments of S2 and S5 are depicted below.

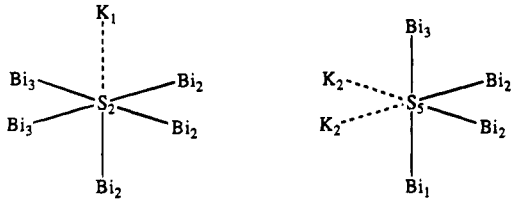

Bi(1) in KBi_3S_5 is in a distorted octahedral coordination with four equatorial bonds at 2.832(8) and 2.823(7) Å and a short axial bond of 2.64(1) Å *trans* to a long bond of 3.10(1) Å. The S(4′)−Bi(1)−S(5) angle of 162.5(3)° suggests that the deviation from a normal 180° angle is caused by the stereochemically active lone pair of Bi. The Bi(2) coordination is also distorted with a short axial distance of 2.66(1) Å, *trans* to a long bond of 3.12 (1) Å. This long−short bond alteration is also seen at the Bi(1,2) sites in $CsBi_3S_5$.[8] A similar environment is found in the naturally occurring bismuth sulfosalts, including Bi(1) in $PbBi_2S_4$[18] and Bi(5) in $PbCu_4Bi_5S_{11}$.[19]

Comparison of the unit cell volumes of KBi_3S_5 (1204 Å^3) with two other related compounds, $CsBi_3S_5$ (1036 Å^3) and α-$RbBi_3S_5$ (991 Å^3), show that KBi_3S_5 possesses the largest volume despite the fact that it contains the smallest alkali ion. This is consistent with the presence of some void space in the crystal. All three compounds have orthorhombic unit cells with the smallest axis being close to 4 Å. Based on the unit cell volumes of the ABi_3S_5 compounds, we expect a dense phase of KBi_3S_5 to have a volume of ~960 Å^3, 20% smaller than that observed. Though we did not encounter the dense-packed version of KBi_3S_5 in our studies, it may exist at higher temperatures, according to earlier claims.[28] The relatively open structure of KBi_3S_5 suggests that the Rb^+ and Cs^+ analogs may be possible under the proper synthetic conditions.

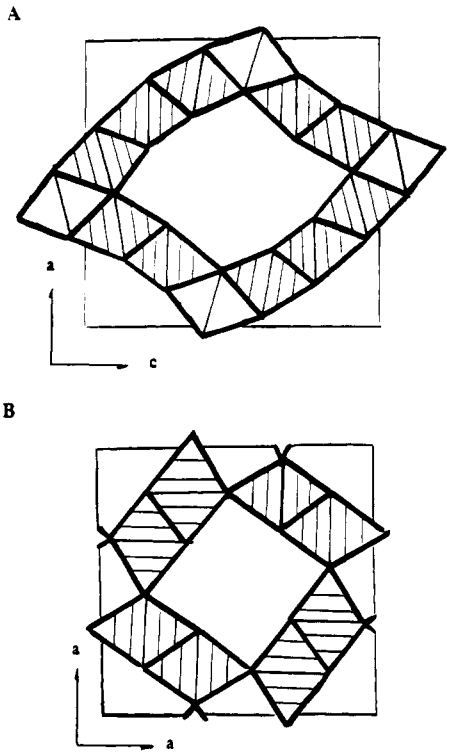

Figure 3. (a) Polyhedral representation of the $[Bi_3S_5]_n^{n-}$ framework projected in the *b*-direction. The octahedra that line the tunnel are shaded. (b) Adapted polyhedral representation of the hollandite anion framework projected in the *c*-direction showing the 2 × 2 tunnel structure.[30c]

The structure of KBi_3S_5 is reminiscent of hollandite which is composed of MO_6 octahedra (M = Ti,[30] Ru,[31] Mo,[32] Mn[33]) linked via edges and corners to form tunnels of various sizes in which alkali and/or alkaline earth metal cations reside. Many of these phases exhibit disorder in the cation sites and have been well-studied because of their ionic conductivity,[34] redox intercalation behavior (α-MnO_2),[35] and ion-exchange properties.[36] Figure 3 shows polyhedral representations of the $[Bi_3S_5]_n^{n-}$ anion and hollandite anion frameworks for comparison. The unit cell of the hollandite structure is tetragonal with a = 9.8 Å and c = 2.86 Å.[37] The tunnels of KBi_3S_5 (14.02 × 9.45 Å) are much larger than those of hollandite (6.6 × 4.7 Å). The hollandite framework, shown in Figure 4b, is made up of chains of MO_6 octahedra that share opposite edges in the *c*-direction. The octahedra from one chain share edges with two consecutive octahedra from the other chain to form double chains in the *c*-direction. The double chains are combined by corner-sharing to form a three-dimensional (2 × 2) framework.

(30) (a) Fanchon, E.; Vicat, J.; Hodeau, J.-L.; Wolfers, P.; Tran Qui, D.; Strobel, P. *Acta Crystallogr.* **1987**, *43B*, 440−448. (b) Fanchon, E.; Vicat, J.; Hodeau, J.-L.; Levy, J.-P.; Wolfers, P. *Acta Crystallogr.* **1987**, *Sect. A 43(Suppl.)*, C-129. (c) Bursill, L. A. *Acta Crystallogr.* **1979**, *B35*, 530−538.

(31) Torardi, C. C. *Mater. Res. Bull.* **1985**, *20*, 705−713.

(32) Torardi, C. C.; McCarley, R. E. *J. Solid State Chem.* **1981**, *37*, 393−397.

(33) Burns, R. G.; Burns, M. B. *Manganese Dioxide Symposium*; Tokyo, 1981; Vol. 2, Chapter 6.

(34) (a) Khanna, S. K.; Gruner, G.; Orbach, R.; Beyeler, H. U. *Phys. Rev. Lett.* **1981**, *47*, 255−257. (b) Beyeler, H. U.; Bernasconi, J.; Strässler, S. *Fast Ion Transport in Solids*; Vashishta, P., Mundy, J. N., Shenoy, G. K., Eds.; North-Holland: New York, 1979; p 503.

(35) Clearfield, A. J. *Chem. Rev.* **1988**, *88*, 125−148.

(36) Shen, X.-M.; Clearfield, A. J. *J. Solid State Chem.* **1986**, *64*, 270−282.

(37) Byström, A.; Byström, A. M. *Acta Crystallogr.* **1979**, *B35*, 530−538.

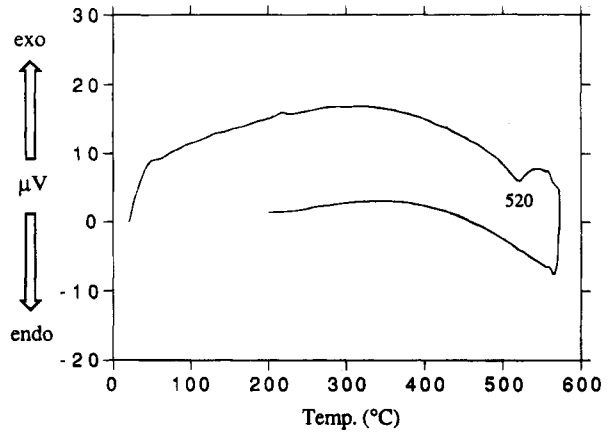

Figure 4. DTA thermogram of KBi_3S_5.

Similarly, the tunnel structure of KBi_3S_5 (Figure 4a) can be viewed as edge-sharing triple chains sharing corners with double chains to form the interior (3 × 2) structure of the tunnel. KBi_3S_5 is also similar to psilomelane ($Ba_xMn_5O_{16}\cdot(2-x)H_2O$, $0.50 < x < 0.75$) and $RbCr_3S_5$ which also contain 3 × 2 tunnel structures.[38] Assuming a van der Waals diameter for sulfur of 3.6 Å the kinetic diameter of these channels is roughly 6−10 Å comparable to a small pore zeolite.

Thermal Analysis. The thermal behavior of KBi_3S_5 was investigated with differential thermal analysis (DTA). Figure 4 shows that upon heating KBi_3S_5, a broad endotherm occurs at 520 °C. Upon cooling, no corresponding exothermic peak is observed suggesting an irreversible change in the structure even though no change in the physical appearance of the compound was observed. Powder X-ray diffraction (XRD) of the heated sample gave a new XRD pattern, perhaps forming β-KBi_3S_5. The low angle (101) peak of KBi_3S_5 shifts from 12.13 to 11.33 Å. The XRD peaks from this, apparently new, phase match those from the minor impurity phase found in the $Bi + 2.8K_2S_{5.3}$ reaction mentioned above but do not match those found for the high temperature K_2S/Bi_2S_3 phases.[28] Further work is needed to characterize this compound.

Ion-Exchange Studies. The relatively open structure of KBi_3S_5 encouraged us to explore possible ion-exchange behavior. For example, ion-exchange studies of KBi_3S_5 were performed in a dilute aqueous HCl solution with the goal of synthesizing a proton-exchanged material. Our first attempt resulted in an air oxidized product which was formulated as "$(H_2O)Bi_3S_{4.5}(S_x)_{0.5/x}$" instead of a truly topotactic ion-exchanged product, $(H_3O)Bi_3S_5$. The reasons for this unusual formulation will become apparent below.

Figure 5 shows the powder X-ray diffraction (XRD) patterns of KBi_3S_5 and "$(H_2O)Bi_3S_{4.5}(S_x)_{0.5/x}$". The low angle peaks of KBi_3S_5 remain after the reaction, indicating that the Bi/S framework is more or less intact. However, a number of additional peaks appear which reveal a possible reduction in symmetry and suggest that the reaction is not really topotactic. Examination of the product with scanning electron microscopy (SEM) shows no change in crystallite size (1−30 μm) and shape suggesting at least a pseudomorphic reaction (see Figure 6).[39]

A thermogravimetric analysis (TGA) diagram of the ion-exchanged product up to 330 °C is shown in Figure 7a. Step I (3.82% weight loss), starting at 140 °C, is due to the loss of

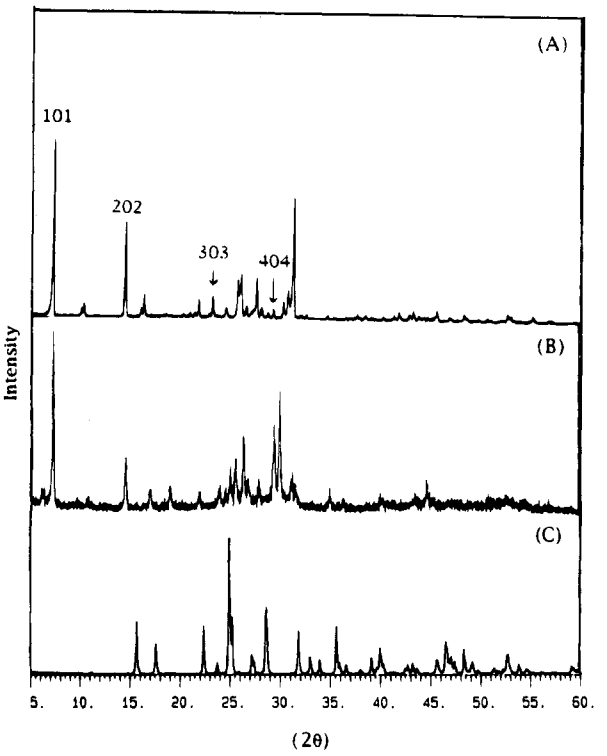

Figure 5. Comparison of the X-ray powder diffraction patterns of (a) KBi_3S_5 with selected *h0l* peaks labeled; (b) "$(H_2O)Bi_3S_{4.5}(S_x)_{0.5/x}$"; and (c) Bi_2S_3.

H_2O as confirmed by mass spectrometry. This is immediately followed by step II (3.84% weight loss), starting at 176 °C, which corresponds to the loss of 1/2 mol of sulfur. The formation of Bi_2S_3 after step II was confirmed by XRD (vide infra). Since the H_2O is not removed until 140 °C, this suggests that H_2O is located inside the tunnels and not on the surface. As a control experiment, KBi_3S_5 was stirred in H_2O for 1 h. The TGA of the product did not show any weight loss up to 400 °C.

The assignment of step II in Figure 7a is supported by the mass spectrum which shows *m/z* peaks corresponding to S_x^+ ($x = 1-8$). The dominant peak is found at *m/z* 64 (S_2^+). The presence of an intense S_2^+ peak during this decomposition is not unreasonable. For example, studies of the complex sulfur vapor equilibra have shown that at temperatures higher than ~320 °C and at pressures lower than ~1 Torr, the vapor phase of sulfur is dominated by the S_2 species.[40] The heating of HgS to 308 °C under low pressure gives S_2^+ as the major ion peak.[41] To determine if the S_8 fragment was located on the surface of the material or inside the tunnels, the material was washed with CS_2 and ether. TGA of the washed product still showed loss of H_2O and an intense S_2^+ peak in the MS spectrum, suggesting that some type of sulfur species (perhaps S_2) is located in the interior of the particles.

Differential scanning calorimetry (DSC) of "$(H_2O)Bi_3S_{4.5}(S_x)_{0.5/x}$" to 400 °C gave a large, sharp endothermic peak at 146 °C followed by a small, broad exothermic peak at 156 °C (see Figure 7b). These thermal events correspond to dehydration, loss of sulfur, and subsequent formation of Bi_2S_3. For comparison, the DSC of KBi_3S_5 performed under identical conditions is featureless.

In order to further characterize the properties of "$(H_2O)Bi_3S_{4.4}(S_x)_{0.5/x}$" the powder XRD pattern was measured as a

(38) (a) Wadsley, A. D. *Acta Crystallogr.* **1953**, *6*, 433−438. (b) Bronger, W.; Herudek, C.; Huster, J.; Schmitz, D. *Z. Anorg. Allg. Chem.* **1993**, *619*, 243−252.

(39) In a pseudomorphic reaction the product retains the morphology of the starting material but (in contrast to a topotactic reaction) its internal crystal and framework structure has been altered.

(40) Liao, C. L.; Ng, C. Y. *J. Chem. Phys.* **1986**, *84*(2), 778−782.

(41) Berkowitz, J. In *Elemental Sulfur*; Meyer, B., Ed.; Interscience: New York, 1965.

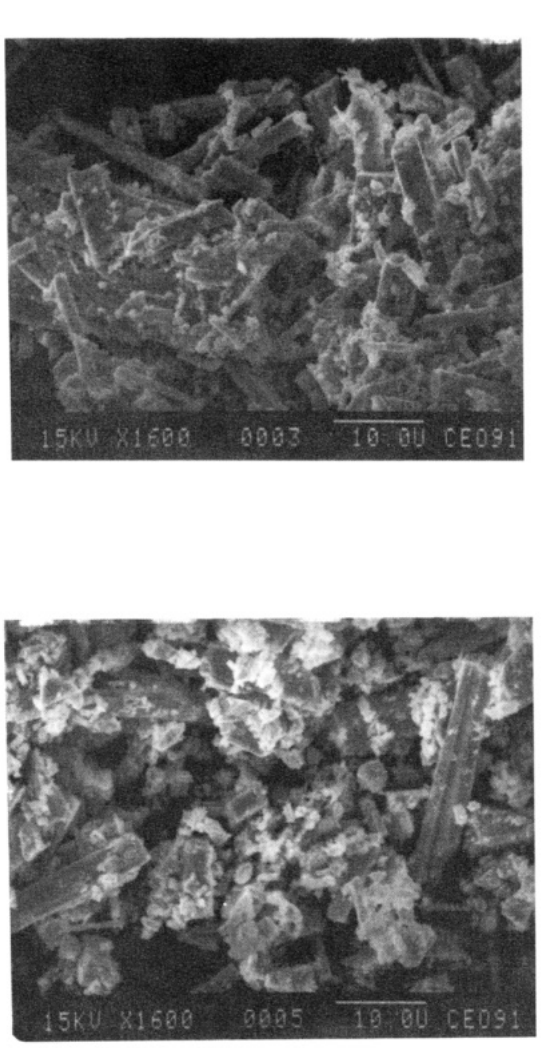

Figure 6. SEM photographs of (a) KBi_3S_5 before and (b) after reaction with aqueous HCl (66 h). The white bar at the bottom of the micrographs represents a 10 μm scale. The magnification is $\times$1600.

function of temperature. Peak broadening was observed with increasing temperature and at 125 °C Bi_2S_3 began to appear. At 145 °C, only broad peaks assignable to Bi_2S_3 were observed. The crystallite size was calculated to be ~160 Å.[42] Heating "$(H_2O)Bi_3S_{4.5}(S_x)_{0.5/x}$" to 80 °C under vacuum for 11 h, resulted in partial decomposition to Bi_2S_3. These data suggest that the framework collapses upon removal of the water and then expels sulfur to form Bi_2S_3.

The mid-IR spectrum of "$(H_2O)Bi_3S_{4.5}(S_x)_{0.5/x}$" did not show any S−S stretching vibrations. Since the proposed concentration of sulfur in the compound is very dilute, it is possible that the intensities of these vibrations are very weak.

Since the ion-exchange chemistry in air gave an oxidation product, the same experiment was carried out under nitrogen atmosphere. Interestingly, the XRD of the product gave the same pattern as KBi_3S_5 with broadened peaks and EDS confirmed the presence of K^+ indicating no appreciable ion-exchange. Clearly, the reaction of KBi_3S_5 with an aqueous HCl solution in air results in the formation of an increasing metastable product. Based on the data presented, Scheme 1 regarding the interaction of KBi_3S_5 with aqueous HCl is proposed.

We also explored cation-exchange reactions with alkali and ammonium ions. Room temperature reactions with aqueous solutions of various salts (NaCl, Rb_2CO_3, CsCl, NH_4NO_3) and methanol solutions of cesium acetate did not show ion-exchange. Hydrothermal treatment of KBi_3S_5 at 130 °C with alkali metal salt solutions of RbCl and CsCl and gave Bi_2Si_3, while methanothermal treatment of KBi_3S_5 at 85 °C with Cs and Na acetate salts did not show ion-exchange.

Solid State Ion-exchange Reactions with Halide Salts. The complications arising from the ion-exchange attempts using solvents prompted us to investigate "dry" reactions with solid alkali halide salts according to eq 1.

$$KBi_3S_5 + ACl \xrightarrow{\Delta} ABi_3S_5 + KCl \qquad (1)$$
$$A = Na, Rb, Cs$$

Solid state topotactic ion-exchange is a very useful synthetic method and has been demonstrated in several systems, including $A_2Mo_6Q_6$ (A = Na, K, Rb, Cs, Cu, Ag; Q = S, Se),[43] $A_xNb_6Q_8$ (A = Na, Rb, K, transition metals; Q = S, Se, Te),[44] AV_5Q_8,[45] and AV_6Q_8 (A = Na, K, Rb, Cs; Q = S, Se, Te).[45] In these systems, the halide salt is heated above its melting point. Because KBi_3S_5 is only kinetically stable, the reaction cannot

(42) Debye-Scherrer formula: $D = (0.9*\lambda*57.3)/(\beta_{1/2}*\cos\theta)$ (D = av crystallite size (Å); λ = radiation wavelength; $\beta_{1/2}$ = peak width at half height; θ = Bragg angle).

(43) Tarascon, J. M.; Hull, G. W.; DiSalvo, F. J. *Mater. Res. Bull.* **1984**, *19*, 915−924.

(44) (a) Huan, G.; Greenblatt, M. *Mater. Res. Bull.* **1987**, *22*, 505−512. (b) Huan, G.; Greenblatt, M. *Mater. Res. Bull.* **1987**, *22*, 943−949.

(45) Ohtani, T.; Sano, Y.; Kodama, K.; Onoue, S.; Nishihara, H. *Mater. Res. Bull.* **1993**, *28*, 501−508.

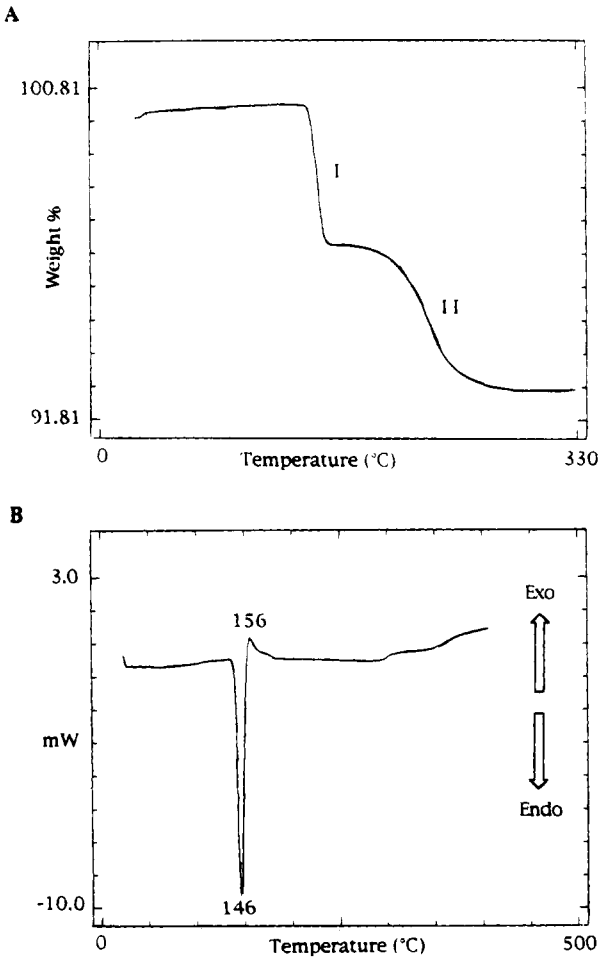

Figure 7. (a) Thermogravimetric analysis plot of "$(H_2O)Bi_3S_{4.5}•(S_x)_{0.5/x}$" with weight % plotted against temperature (°C): performed under flowing N_2, step I (3.82% weight loss starting at 140 °C), step II (3.84% weight loss starting at 176 °C). (b) DSC thermogram of "(H_2O)-$Bi_3S_{4.5}•(S_x)_{0.5/x}$".

Scheme 1

$$[Bi_3S_5]^- + {}^1/_4O_2 + H_3O^+ \longrightarrow "(H_2O)Bi_3S_{4.5}•(S_x)_{0.5/x}" + {}^1/_2H_2O$$

$$\Delta \downarrow -H_2O$$

$$^3/_2Bi_2S_3 \xleftarrow[-{}^1/_{16}S_8]{\Delta} "Bi_3S_{4.5}•(S_x)_{0.5/x}"$$

be heated above the melting point (>700 °C) of either NaCl, RbCl, or CsCl. It is therefore remarkable that in the RbCl case, complete topotactic ion-exchange occurs below 400 °C forming the isostructural β-$RbBi_3S_5$ (see Table 1). At or above 400 °C the known denser phase α-$RbBi_3S_5$[4] forms, confirming that both KBi_3S_5 and β-$RbBi_3S_5$ are only kinetically stable structures and thus metastable. The fact that this relatively facile ion-exchange reaction is a solid–solid reaction suggests that the exchanging ions possess high ionic mobilities probably promoted by the large tunnels present in the $[Bi_3S_5]^-$ structure.[46] This suggests that the ABi_3S_5 may be good ionic conductors. The β-phase possesses higher symmetry because the split peaks that are seen at low angles in KBi_3S_5 are single peaks in β-$RbBi_3S_5$ suggesting a possible transformation to a tetragonal structure. Interestingly, β-$RbBi_3S_5$ could not be synthesized by the molten alkali polysulfide approach.

Unfortunately, preliminary reactions with NaCl (200–400 °C) resulted in a mixture of $NaBiS_2$ and Bi_2S_3. The Na^+ ion may be too small to support the $[Bi_3S_5]^-$ framework at this temperature. Reactions with CsCl gave a mixture of the layered γ-$CsBiS_2$[19] and a minor impurity phase. Elemental EDS analysis on several 10 μm needles gave a composition $CsBi_{3.1}S_{5.2}$; analysis on the 10 μm plates gave $CsBi_{2.5}S_{3.4}$. XRD of the mixture did not reveal the presence of $CsBi_3S_5$.[3] Ion-exchange reactions with solid NH_4Cl and NH_4I (150–400 °C) gave Bi_2S_3 and H_2S, suggesting HBi_3S_5 as a possible intermediate.

Concluding Remarks

The isolation of KBi_3S_5 from a polysulfide flux at a relatively low temperature confirms the usefulness of molten salts in low enough temperatures for the stabilization of reactive solid state materials. Although the void space within this metastable material is not substantial, KBi_3S_5 represents a rare example of a chalcogenide with an open framework and ion-exchange properties. This and other materials provide the basis for further exploratory work to identify not only new open framework chalcogenides but also a reliable general synthetic methodology to these materials. Such a methodology could be greatly aided by drawing lessons from the recent preparative successes in the more familiar zeolites,[47] aluminosilicates (MCM-41),[48] and pillared clays.[49]

Acknowledgment. Financial support from the National Science Foundation CHE 92-24102 (Chemistry Research Group) is gratefully acknowledged. The X-ray instrumentation used in this work was purchased in part with funds from the National Science Foundation (CHE-89-08088). We thank Mr. Rabin Bissessur and Dr. Rui Huang for assistance with the variable temperature XRD experiment. We also thank Chris Petty of Nicolet Instrument Corp. for recording the Raman spectrum of KBi_3S_5. This work made use of the SEM facilities of the Center for Electron Optics at Michigan State University.

Supplementary Material Available: Tables of atomic coordinates of all atoms and ansiotropic and isotropic thermal parameters of all non-hydrogen atoms and bond distances and angles (6 pages); a listing of calculated and observed ($10F_o$/$10F_c$) structure factors (6 pages). This material is contained in many libraries on microfiche, immediately follows this article in the microfilm version of the journal, and can be ordered from the ACS; see any current masthead page for ordering information.

JA941303U

(46) Even though this remarkable reaction appears to proceed at the solid to solid interface at such a low temperature, one may also imagine the presence of a liquid phase covering the surface of the KBi_3S_5 particles. However no eutectic composition between KCl and RbCl is known below 700 °C.

(47) Ozin, G. A. *Adv. Mater.* **1992**, *4*, 612–649.
(48) Kresge, C. T.; Leonowicz, M. E.; Roth, W. J.; Vartuli, J. C.; Beck, J. S. *Nature* **1992**, *359*, 710–712.
(49) Pinnavaia, T. J. *Science* **1983**, *220*, 365–371.